



Acidity of titania-supported tungsten or niobium oxide catalysts Correlation with catalytic activity

Thomas Onfroy ^a, Guillaume Clet ^a, Saeed B. Bukallah ^b,
Tom Visser ^c, Marwan Houalla ^{a,*}

^a Laboratoire Catalyse et Spectrochimie, UMR CNRS 6506, ENSICAEN-Université de Caen, 6 Bd. du Maréchal Juin,
14050 Caen Cedex, France

^b Surface Sciences and Applied Catalysis, Faculty of Sciences, Chemistry Dept., UAE University,
P.O. Box 17551, Al-Ain, UAE

^c Department of Inorganic Chemistry and Catalysis, Debye Institute, Utrecht University, Sorbonnelaan 16,
3584 CA Utrecht, The Netherlands

Received 20 July 2005; received in revised form 13 September 2005; accepted 22 September 2005
Available online 9 November 2005

Abstract

The acidity of catalytic systems based on tungsten oxide or niobium oxide supported on titania was compared. Two series with metal contents up to 3.6 atom nm⁻² were prepared by incipient wetness impregnation of the titania support with ammonium metatungstate or niobium oxalate solutions. Characterization of both systems by X-ray diffraction and Raman spectroscopy studies did not show evidence of bulk metal oxide formation. The acidity was monitored by adsorption of 2,6-dimethylpyridine (2,6-lutidine) followed by infrared spectroscopy. The catalytic activity was tested for the reaction of isopropanol dehydration.

At a reaction temperature of 403 K, WO_x/TiO₂ catalysts were inactive for a surface density of W ≤ 1.2 W atom nm⁻². Above this loading, the activity increased progressively with increasing W content. Similar evolution was observed for the abundance of relatively strong Brønsted acid sites (i.e. able to retain lutidine at 573 K). In contrast, NbO_x/TiO₂ catalysts were essentially inactive at this reaction temperature and a higher reaction temperature (473 K) was required to reach a comparable catalytic activity. No threshold of Nb loading for the development of catalytic activity was observed. Similar behavior was evidenced for the abundance of medium strength Brønsted acid sites (able to retain lutidine at 523 K). For both systems, a direct correlation between the catalytic activity and the abundance of Brønsted acid sites was observed.

© 2005 Elsevier B.V. All rights reserved.

Keywords: Acidity; Titania-supported tungsten oxide; Titania-supported niobium oxide; Propanol dehydration; 2,6-Dimethyl pyridine adsorption

1. Introduction

Supported metal oxides of the groups 5 and 6 often show acidic properties. To understand the genesis of the acidity, it is of interest to investigate the role of the support and the supported phase in determining the nature, force and abundance of the acid sites. Supported W oxides have been widely studied for acid-catalyzed reactions such as alkenes [1,2] or alkanes [3–5] isomerization. Several acid-catalyzed reactions were also reported for the corresponding Nb-based systems [6–11].

In previous studies, we have shown that both tungsten [12,13] and niobium [14,15] oxides supported on zirconia induce the formation of Brønsted acid sites. For both systems significant formation of Brønsted acid sites only occurs above a threshold of W or Nb surface density of about 1.2 atom nm⁻². Similar evolution was observed for the catalysts activity for propanol dehydration. However, a large difference in the catalytic performance was observed, which was attributed to the presence of relatively stronger Brønsted acid sites for the W system.

The purpose of the present paper is to examine how the above noted characteristics of both systems (presence of a threshold of W or Nb loading for the appearance of Brønsted acid sites; evolution of the acidity with the surface density of deposited metal oxide; correlation with activity for acid-

* Corresponding author. Tel.: +33 2 31 56 73 51; fax: +33 2 31 45 28 22.
E-mail address: Marwan.Houalla@ensicaen.fr (M. Houalla).

catalyzed reaction) are affected by the nature of the support. Towards this objective, the surface structure and catalytic properties of titania-supported W and Nb systems will be examined. These systems have also been shown to exhibit acidic properties [5,10,11,16–21]. Characterization of both systems will be conducted by X-ray diffraction and Raman spectroscopy studies. The acidity will be monitored by adsorption of 2,6-dimethylpyridine (2,6-lutidine or DMP) followed by infrared spectroscopy. The results will be correlated with catalytic activity for the reaction of isopropanol dehydration.

2. Experimental

2.1. Preparation of the solids

The titania support (Degussa; P-25) was previously calcined at 823 K for the W system and at 673 K for the niobium-containing solids. Supported catalysts were prepared by incipient wetness impregnation of the TiO_2 support with a solution of the metal precursor. For WO_x/TiO_2 , the support was impregnated with an aqueous solution of ammonium metatungstate ($(\text{NH}_4)_6\text{H}_2\text{W}_{12}\text{O}_{40}$) then dried at 393 K for 16 h and calcined in air at 773 K for 16 h. For $\text{NbO}_x/\text{TiO}_2$, the support was impregnated with a mixture of 7 wt.% of niobium (V) oxalate and 93 wt.% of oxalic acid diluted in the required amount of water, dried at 393 K for 16 h and calcined in air at 723 K for 16 h.

Supported tungsten and niobium oxides will be designated as W_xT and Nb_yT , respectively, where x and y represent the metal (W or Nb) density in atom nm^{-2}

2.2. BET surface area

Nitrogen adsorption was measured at 77 K with an automatic adsorptiometer (Micromeritics ASAP 2000). The samples were pre-treated at 573 K for 2 h under vacuum. The surface areas were determined from adsorption values at five relative pressures (P/P_0) ranging from 0.05 to 0.2 using the BET method. The pore volumes were determined from the total amount of N_2 adsorbed between $P/P_0 = 0.05$ and 0.98.

2.3. X-ray diffraction

X-ray powder diffraction spectra were recorded using a Philips X'pert diffractometer with copper anode ($\text{K}\alpha_1 = 0.15405 \text{ nm}$) and a scanning rate of $0.025^\circ \text{ s}^{-1}$. The anatase/rutile composition of the support was determined from the intensities of the peaks I_A and I_R characteristics of the (1 0 1) plane of anatase and the (1 1 0) plane of rutile located, respectively, at $2\theta = 25.4^\circ$ and 27.5° , using the following formula [22]:

$$A = \frac{1}{1 + 1.26 \frac{I_R}{I_A}}$$

where A designates the fraction of the support present as anatase.

2.4. Raman spectroscopy

Raman characterization was performed under ambient conditions. The spectra (20 scans of 10 s; resolution 2 cm^{-1}) were recorded with a dispersive Raman (Kaiser) equipped with diode laser source ($\lambda = 532 \text{ nm}$) and a CCD camera.

2.5. Infrared spectroscopy

The samples, pressed into pellets ($\sim 20 \text{ mg}$ for a 2 cm^2 pellet), were first heated under vacuum at 623 K for 30 min. This first treatment was followed by a treatment in O_2 ($P_{\text{equilibrium}} = 13.3 \text{ kPa}$) for 1 h, and evacuation for 30 min at 623 K before cooling down to room temperature (295 K).

IR spectra were recorded with a Nicolet Magna 550 FT-IR spectrometer (resolution: 4 cm^{-1} , 128 scans). All the spectra shown in the present study were obtained after subtraction of the spectra of evacuated sample and normalization for 100 mg of the solid. 2,6-Dimethylpyridine was introduced at 295 K ($P_{\text{equilibrium}} = 133 \text{ Pa}$), after activation. Spectra were then recorded after desorption from 323 to 573 K. The cell was evacuated at the desorption temperature until a residual pressure below $6.7 \times 10^{-4} \text{ Pa}$. The abundance of Brønsted acid sites titrated by 2,6-dimethyl pyridine was estimated from the sum of the bands at 1643 and 1627 cm^{-1} (respectively, v_{8a} and v_{8b} vibrations) using a previously determined [23] value of the integrated molar absorption coefficient (ε) of the vibrations ($v_{8a} + v_{8b}$) of protonated lutidine (DMPH^+): $\varepsilon = 6.8 \text{ cm } \mu\text{mol}^{-1}$.

2.6. Catalytic activity

The catalytic conversion of propan-2-ol (isopropanol) was measured in a fixed bed flow reactor. Hundred milligrams of sample was pre-treated at 723 K in N_2 for 2 h (ramp 5 K min^{-1} ; $60 \text{ cm}^3 \text{ min}^{-1}$). The reaction was performed at atmospheric pressure with N_2 as carrier gas ($P_{\text{isopropanol}} = 1.23 \text{ kPa}$; $\text{WHSV} = 17.3 \text{ mmol h}^{-1} \text{ g}^{-1}$; total flow rate = $60 \text{ cm}^3 \text{ min}^{-1}$) at 403 K for WO_x/TiO_2 and 473 K for $\text{NbO}_x/\text{TiO}_2$. Reactants and products were analyzed with an on line G.C. (HP 5890 Series II) equipped with a capillary column (CP WAX 52 CB) and a FID detector.

3. Results

3.1. Preparation of the catalysts

Both WO_x/TiO_2 and $\text{NbO}_x/\text{TiO}_2$ series were prepared by incipient wetness impregnation of the titania support with a solution of the metal salts deposited on titania. Two series of solids containing up to 4.8 wt.% of metal (3.4 atom nm^{-2}) were obtained. The characteristics of the solids are summarized in Table 1 for the tungsten-containing solids and in Table 2 for the niobium-containing system. TiO_2 had a surface area of $46 \text{ m}^2 \text{ g}^{-1}$ and a pore volume equal to $0.24 \text{ cm}^3 \text{ g}^{-1}$. For all the supported solids, the specific surface area of the support was not modified significantly on metal addition. The surface density was, thus, expressed as the number of atoms of Nb or W

Table 1
Characteristics of WO_x/TiO_2 catalysts

	Sample						
	TiO_2	W0.6 T	W1.1 T	W1.7 T	W2.3 T	W2.8 T	W3.4 T
W (wt.%)	0.00	0.80	1.60	2.40	3.20	4.00	4.80
WO_3 (wt.%)	0.00	1.01	2.02	3.03	4.04	5.05	6.06
W (atom nm^{-2})	0.0	0.6	1.1	1.7	2.3	2.8	3.4
% Monolayer	0	12	22	35	47	57	69
Surface area ($\text{m}^2 \text{g}^{-1}$)	46	47	47	47	47	47	46
Pore volume ($\text{cm}^3 \text{g}^{-1}$)	0.24	0.25	0.24	0.25	0.24	0.23	0.24
% Anatase	58	60	58	59	61	63	57

Table 2
Characteristics of $\text{NbO}_x/\text{TiO}_2$ catalysts

	Sample				
	TiO_2	Nb0.6 T	Nb1.2 T	Nb2.4 T	Nb3.6 T
Nb (wt.%)	0.00	0.48	0.95	1.88	2.79
Nb_2O_5 (wt.%)	0.00	0.69	1.36	2.69	3.99
Nb (atom nm^{-2})	0.0	0.6	1.2	2.4	3.6
% Monolayer	0	10	20	40	60
Surface area ($\text{m}^2 \text{g}^{-1}$)	46	45	46	46	48
Pore volume ($\text{cm}^3 \text{g}^{-1}$)	0.24	0.24	0.23	0.23	0.26
% Anatase	62	59	60	62	61

per nm^2 of the titania support. For WO_x/TiO_2 , the theoretical coverage was calculated assuming that a full monolayer corresponds to $4.9 \text{ W atom nm}^{-2}$ [24,25]. For $\text{NbO}_x/\text{TiO}_2$, the theoretical coverage was estimated considering that each Nb_2O_5 unit occupies 0.32 nm^2 [26].

3.2. X-ray diffraction

The diffraction pattern of TiO_2 showed two main peaks at $2\theta = 25.4^\circ$ and 27.5° , characteristic, respectively, of the (1 0 1) plane of anatase and the (1 1 0) plane of rutile [22,27]. The composition of the support was 60% anatase–40% rutile. The percentage of anatase in the support reported in Tables 1 and 2 was estimated from the relative intensity of these peaks (see Section 2). No significant change in the composition of the titania support (anatase/rutile ratio) was observed on deposition of W or Nb. In addition, no peaks, which can be attributed to crystalline WO_3 or Nb_2O_5 , were evidenced.

3.3. Raman spectroscopy

Figs. 1 and 2 show the Raman spectra for the supported WO_x/TiO_2 and $\text{NbO}_x/\text{TiO}_2$ systems, respectively. Also included in these figures is the Raman spectrum of the titania support. The bands located at 396 , 515 and 636 cm^{-1} are characteristic of anatase (A); that observed at 447 cm^{-1} and the shoulder at ca. 605 cm^{-1} are ascribed to rutile (R) [20,26]. The band at 794 cm^{-1} is due to the first overtone vibration of the anatase band at 396 cm^{-1} [28]. In accord with XRD results, the addition of metal oxide on the titania support did not modify significantly the relative intensities of these bands, indicating

that the composition of the support was not affected by the deposition of the supported phase.

For W-containing solids (Fig. 1), Raman spectra show the presence of a band between 950 and 975 cm^{-1} characteristic of surface W species [19,20,29–31] and attributed to the vibration of $\text{W}=\text{O}$ bond in hydrated mono-oxotungstate species on titania surface [18,31]. No bands indicative of the presence of bulk WO_3 (bands at 806 and 713 cm^{-1}) were detected.

As suggested by XRD results, Raman spectra of $\text{NbO}_x/\text{TiO}_2$ samples (Fig. 2) did not indicate the presence of Nb_2O_5 (a band at ca. 675 cm^{-1} [32] for hexagonal Nb_2O_5 and around 260 cm^{-1} for monoclinic Nb_2O_5 [32,33]). Niobic acid ($\text{Nb}_2\text{O}_5 \cdot n\text{H}_2\text{O}$) is characterized by a wide band around 650 cm^{-1} [26,32]. The detection of this band in titania-supported catalysts is hindered by the presence of a large band at 636 cm^{-1} due to anatase.

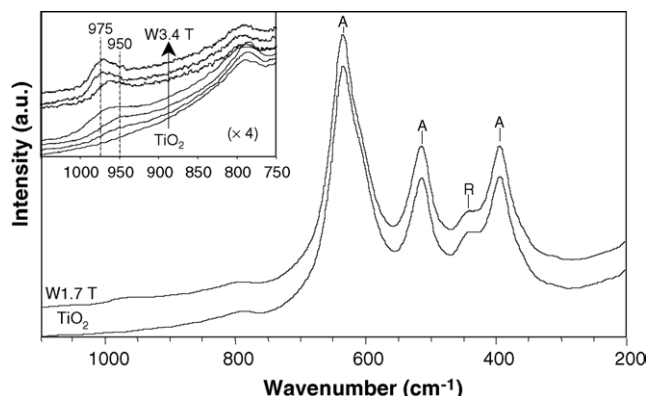


Fig. 1. Raman spectra of TiO_2 and $\text{W}1.7 \text{ T}$ catalysts under ambient conditions, normalized to the 636 cm^{-1} band. Inset: Enlargement of the 1050 – 750 cm^{-1} region for TiO_2 and WO_x/TiO_2 solids.

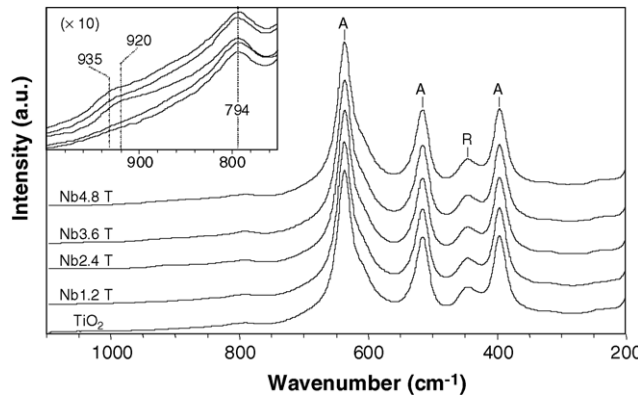


Fig. 2. Raman spectra of NbO_x/TiO₂ catalysts under ambient conditions, normalized to the 636 cm⁻¹ band, between 1100 and 200 cm⁻¹. Inset: Enlarge-ment of the 1000–750 cm⁻¹ region.

Subtracting the contribution of the titania support as proposed by Pittman et al. [26] did not reveal the presence of the niobic acid phase.

Analysis of the Raman spectra in the 750–1100 cm⁻¹ region showed the presence of a weak and broad band located at ca. 920 cm⁻¹ for low Nb loadings which shifts towards 935 cm⁻¹ with increasing metal content. This band was attributed to a hydrated niobate surface species [34].

3.4. Infrared spectroscopy

Fig. 3a shows the infrared spectra for the titania support following adsorption of 2,6-lutidine (at 133 Pa) and desorption at 423 K. In agreement with Lahousse et al. [35] and Travert et al. [36], a doublet is observed at 1643 and 1627 cm⁻¹ characteristic of the v_{8a} and v_{8b} , vibrations of protonated lutidine and due to Brønsted acid sites, and a band at 1614 cm⁻¹ characteristic of lutidine adsorbed on Lewis acid sites. Also shown in Fig. 3a are the infrared spectra of WO_x/TiO₂ under the same conditions. It can be readily seen that the abundance of Lewis acid sites decreased with increasing W

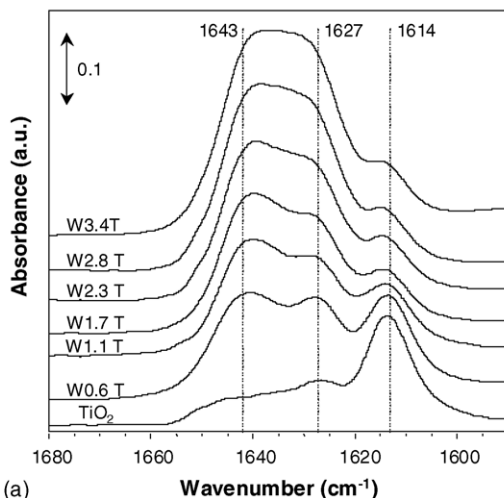


Fig. 3. Adsorption of lutidine on WO_x/TiO₂ catalysts: (a) IR spectra of TiO₂ and WO_x/TiO₂ after desorption of lutidine at 423 K (spectra normalized for 100 mg); (b) evolution of the abundance of Brønsted acid sites vs. W content, following desorption of lutidine at 423 K (■), 523 K (□) and 573 K (●).

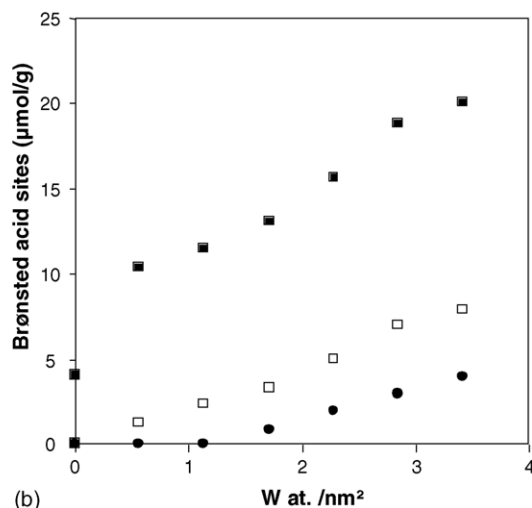
content. This trend is accompanied by a progressive increase in the number of Brønsted acid sites. Fig. 3b shows the evolution of these Brønsted acid sites after desorption at 423, 523 and 573 K. At 423 and 523 K, the concentration of these sites increased linearly with increasing W surface density up to 3.4 W atom nm⁻². However, at the latter temperature, the Brønsted acidity of the titania support was too weak to retain the probe. Following desorption at 573 K, only the solids containing more than 1.1 W atom nm⁻² showed Brønsted acid sites sufficiently strong to retain lutidine. For higher loadings, the abundance of these sites increased linearly with W content.

The infrared spectra of NbO_x/TiO₂ catalysts following adsorption of lutidine and desorption at 423 K are shown on Fig. 4a. As for the W system, Nb addition decreases the number of Lewis acid sites and brings about a progressive increase in the abundance of Brønsted acid sites. The evolution of the Brønsted sites with Nb surface density following desorption at 423, 523 and 573 K is depicted in Fig. 4b. At 423 and 523 K, the observed behavior was similar to that of the corresponding W system. However, following desorption at 573 K, in contrast with the W-based catalysts, no bands characteristic of protonated lutidine were detected.

3.5. Catalytic activity

Both series of solids were tested for the dehydration of propan-2-ol. In this reaction, the formation of propene is correlated to the acidic character. Due to a large difference of activity, W-containing solids were tested at 403 K, whereas the activity of Nb-containing solids was measured at a higher reaction temperature (473 K). The titania support was inactive at 403 K and only slightly active at 473 K (propene formation rate of 0.1 mmol h⁻¹ g⁻¹), which is coherent with previous results by Lahousse et al. [35].

Propene and diisopropyl ether were the only products obtained, acetone was not observed. Hence, both series show an acidic character. For W-based system, at 403 K, the selectivity to propene was about 90%. With Nb-containing solids, at



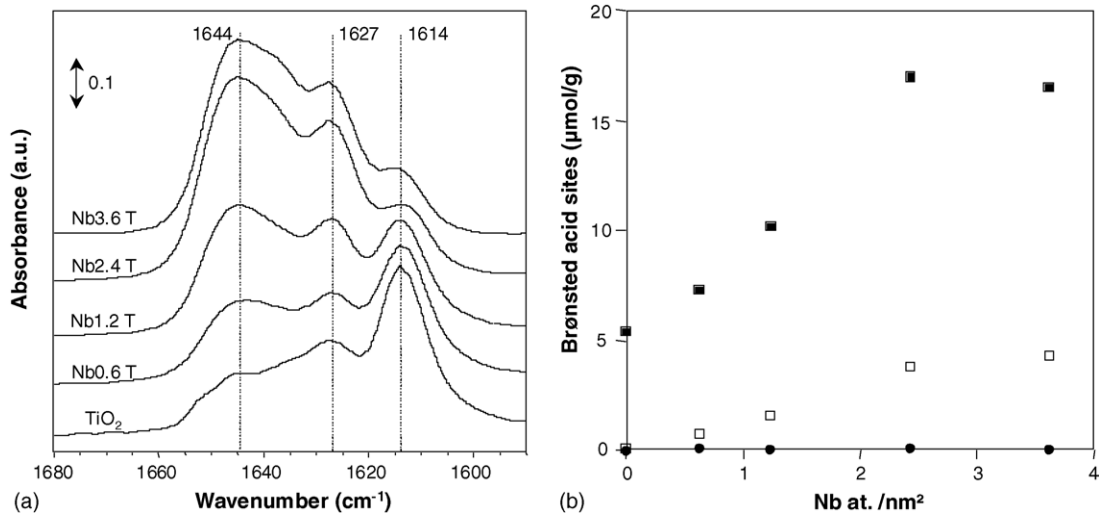


Fig. 4. Adsorption of lutidine on $\text{NbO}_x/\text{TiO}_2$: (a) IR spectra of TiO_2 and $\text{NbO}_x/\text{TiO}_2$ after desorption of lutidine at 423 K (spectra normalized for 100 mg); (b) evolution of the abundance of Brønsted acid sites vs. Nb content, after desorption of lutidine at 423 K (■), 523 K (□) and 573 K (●).

473 K, propene, which is thermodynamically favored at high temperature, was the only product detected.

Fig. 5 presents the propene formation rate for both WO_x/TiO_2 and $\text{NbO}_x/\text{TiO}_2$ series. At 403 K, W-containing solids were inactive below a W surface density of $1.1 \text{ W atom nm}^{-2}$. For higher W loadings, the activity developed progressively to reach $4.5 \text{ mmol h}^{-1} \text{ g}^{-1}$ for $\text{W}3.4 \text{ T}$ (Fig. 5a). For $\text{NbO}_x/\text{TiO}_2$ catalysts (Fig. 5b), as noted above, the titania support exhibited some activity at 473 K. Nb deposition led to a steady increase in activity. In variance with the WO_x/TiO_2 system, no apparent minimum of Nb loading was required for the development of the activity.

4. Discussion

4.1. WO_x/TiO_2

Lutidine adsorption results monitored by infrared spectroscopy indicated that the abundance of Lewis acid sites initially

present on the titania support decreases on deposition of tungsten. This trend is accompanied by the formation of Brønsted acid sites. The detection of Brønsted acid sites in WO_x/TiO_2 is in agreement with previous infrared studies of ammonia [16–20], pyridine [18] and CO adsorption [5,16].

Brønsted acid sites were evidenced in all W-containing solids following desorption of lutidine at 423 and 523 K. The concentration of these sites appears to increase progressively with increasing W content. However, after desorption at 573 K, Brønsted acid sites that are sufficiently strong to retain lutidine at this temperature were only detected for solids above a threshold of W surface density equal to $1.1 \text{ W atom nm}^{-2}$.

Consistent with high temperature lutidine desorption data, a minimum of W loading of $1.1 \text{ W atom nm}^{-2}$ was required for the onset of catalytic activity for isopropanol dehydration at 403 K. Further, analysis of the activity results indicated that this threshold of W coincides with that observed for the formation of relatively strong Brønsted acid sites. The overall evolution of

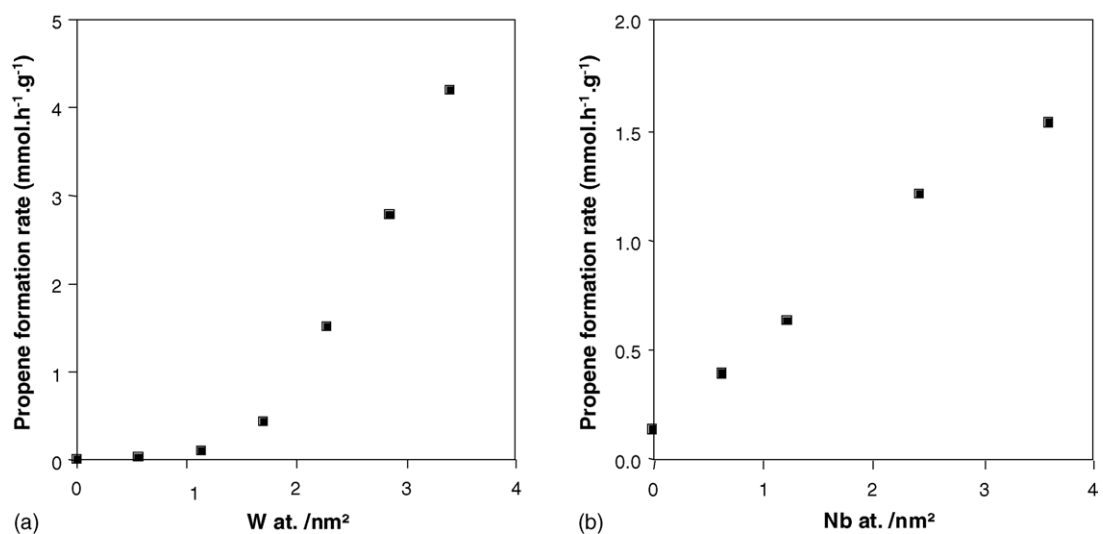


Fig. 5. Propene formation rate vs. metal loading: (a) WO_x/TiO_2 catalysts ($T = 403 \text{ K}$) and (b) $\text{NbO}_x/\text{TiO}_2$ catalysts ($T = 473 \text{ K}$).

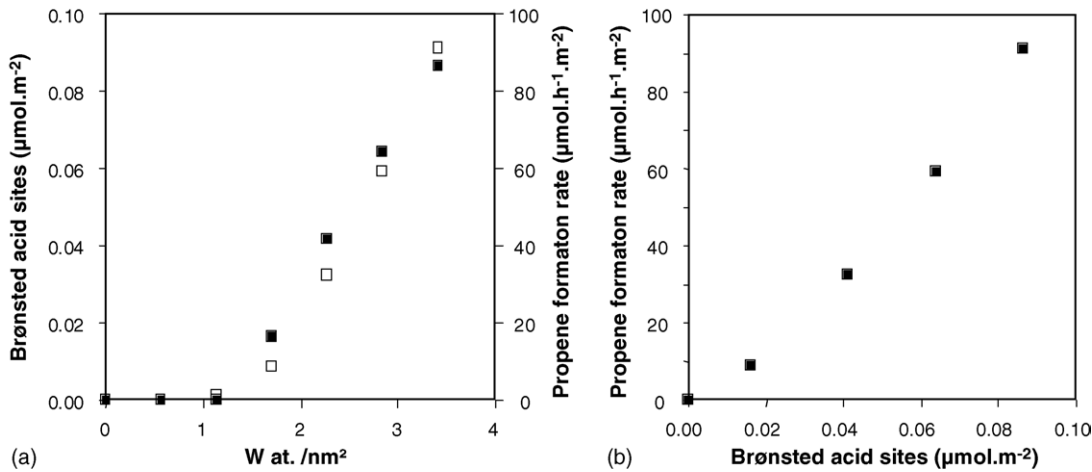


Fig. 6. (a) Propene formation rate at 403 K (□) and abundance of strong Brønsted acid sites determined by desorption of lutidine at 573 K (■) vs. W density of WO_x/TiO_2 catalysts; (b) propene formation rate vs. abundance of Brønsted acid sites for WO_x/TiO_2 catalysts.

the catalytic activity as a function of W surface density was similar to that observed for Brønsted acidity detected by lutidine desorption experiments at 573 K (Fig. 6a). Catalysts containing less than 1.1 W atom nm^{-2} were essentially inactive. Above this loading, propene formation activity developed progressively with W content. The presence of a threshold of W content for the development of activity in an acid-catalyzed reaction (cumene dealkylation) was reported for solids obtained by impregnation of titanium oxyhydroxide and calcined at 773 K [37]. To the best of our knowledge, no such behavior was reported for catalysts obtained by impregnation of titania. It was, however, observed for another type of reaction, i.e. the selective catalytic reduction (SCR) of NO [20] where the Brønsted acidity of the solids has been shown to be an important parameter in determining the overall catalytic performance.

4.2. $\text{NbO}_x/\text{TiO}_2$

As observed in the case of W-based systems, Brønsted acid sites were also evidenced in $\text{NbO}_x/\text{TiO}_2$ catalysts. For a given

Nb surface density, the drastic decrease in the abundance of these sites on increasing the desorption temperature from 423 to 523 K indicates that most of the sites titrated at 423 K are weak in nature. The absence of bands characteristic of protonated lutidine following desorption at 573 K implies that essentially moderate Brønsted acidities are measured following desorption at 523 K. The weak and moderate Brønsted acidity inferred from lutidine desorption results at 423 or 523 K, increased in abundance with Nb loading. The detection of relatively large amounts of Brønsted acid sites is in variance with previous reports by Datka et al. [21] relative to pyridine adsorbed on supported Nb systems where no significant Brønsted acid sites formation had been observed. However, as in the case of zirconia [14,15], this apparent discrepancy can be readily explained by the use in the present study of lutidine which is inherently a more sensitive probe molecule than pyridine for the detection of Brønsted acid sites [23].

Fig. 7a shows the evolution of the number of Brønsted acid sites measured by desorption of lutidine at 523 K, compared to

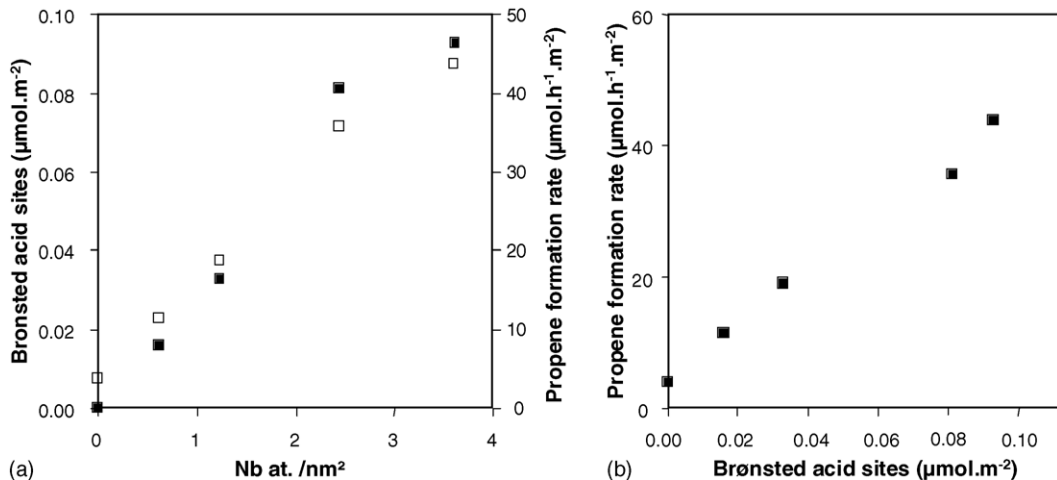


Fig. 7. (a) Propene formation rate at 473 K (□) and abundance of weak Brønsted acid sites determined by desorption of lutidine at 523 K (■) vs. Nb density of $\text{NbO}_x/\text{TiO}_2$ catalysts; (b) propene formation rate vs. abundance of Brønsted acid sites for $\text{NbO}_x/\text{TiO}_2$ catalysts.

that of propene formation rate. For these solids, catalytic activity at 473 K appears to be related to the amount of Brønsted acid sites of medium acidity (obtained after lutidine desorption at 523 K). This relationship can be attributed to the fact that since the reaction is carried out at higher temperature, moderate acidity is probably sufficient to achieve propanol dehydration.

4.3. Comparison of the two systems

4.3.1. Influence of the supported metal loading

The catalytic activity of WO_x/TiO_2 and $\text{NbO}_x/\text{TiO}_2$ catalysts was measured, respectively, at 403 and 473 K (Fig. 5). The W-containing system exhibited a behavior similar to that reported for the zirconia-supported WO_x and NbO_x systems [12–15], namely, the presence of a threshold of W surface density for the appearance and development of activity, followed by a steady increase in activity with increasing W surface density. In contrast, no such threshold was observed for the $\text{NbO}_x/\text{TiO}_2$ system. Up to $3.4 \text{ Nb atom nm}^{-2}$, the rate of propene formation increases progressively with increasing Nb content (Fig. 5b).

The study of the development of Brønsted acidity of both systems with W or Nb surface density indicates a parallel evolution to that of the rate of propene formation (Figs. 6a and 7a). This similarity is illustrated in Figs. 6b (WO_x/TiO_2) and 7b ($\text{NbO}_x/\text{TiO}_2$), which show a direct relation between the abundance of Brønsted acid sites determined by desorption of lutidine and the rate of formation of propene. Thus, the absence of threshold of Nb surface density for the development of catalytic activity noted for the $\text{NbO}_x/\text{TiO}_2$ is reflected in a similar development of Brønsted acid sites. The direct relation between the abundance of Brønsted acid sites and the rate of propene formation suggests that the catalytic activity at a given temperature is associated with the abundance of Brønsted acid sites. This observation is consistent with our previous study of zirconia-supported W [13] and Nb [15] systems where a direct

relation between the evolution of these two parameters has been evidenced.

4.3.2. Influence of the nature of the supported phase

As previously indicated, because of the drastic difference in the catalytic performance of W and Nb systems, the activity measurements were conducted, respectively, at 403 and 473 K. At 403 K, the rate of propene formation for Nb-based catalysts was essentially negligible (Fig. 8a). The important difference in the activity of the two systems (ca. two orders of magnitude) may be attributed, in part, to the difference in the strength of Brønsted acid sites. In effect, lutidine desorption results at 573 K (Fig. 8b) indicate that only catalysts active at 403 K (Fig. 8a) exhibited relatively strong Brønsted acidity (i.e. capable of retaining lutidine at 573 K). In contrast, catalysts inactive at this temperature do not exhibit such sites. Note that these observations are consistent with previous results from our group relative to the zirconia-supported W and Nb systems [15].

4.3.3. Molecular structure of W and Nb species: origin of the active site

The characterization of WO_x/TiO_2 and $\text{NbO}_x/\text{TiO}_2$ by XRD and Raman spectroscopy indicates the absence of bulk WO_3 and Nb_2O_5 phases. Only bands attributed to surface tungstates and niobates were detected (Figs. 1 and 2). In a previous study of WO_x/ZrO_2 [13] and $\text{NbO}_x/\text{ZrO}_2$ [15] systems, the creation and development of Brønsted acid sites were associated with the appearance and development of “extensively” polymerized surface tungstates and niobates. In line with this interpretation, one can propose that in the case of the corresponding titania-supported systems, Brønsted acid sites active for the reaction of isopropanol dehydration are equally associated with the presence and development of these species. The difference in the observed behavior of the $\text{NbO}_x/\text{TiO}_2$ (i.e. absence of minimum loading for the appearance and development of the catalytic activity and Brønsted acidity) can, thus, be attributed

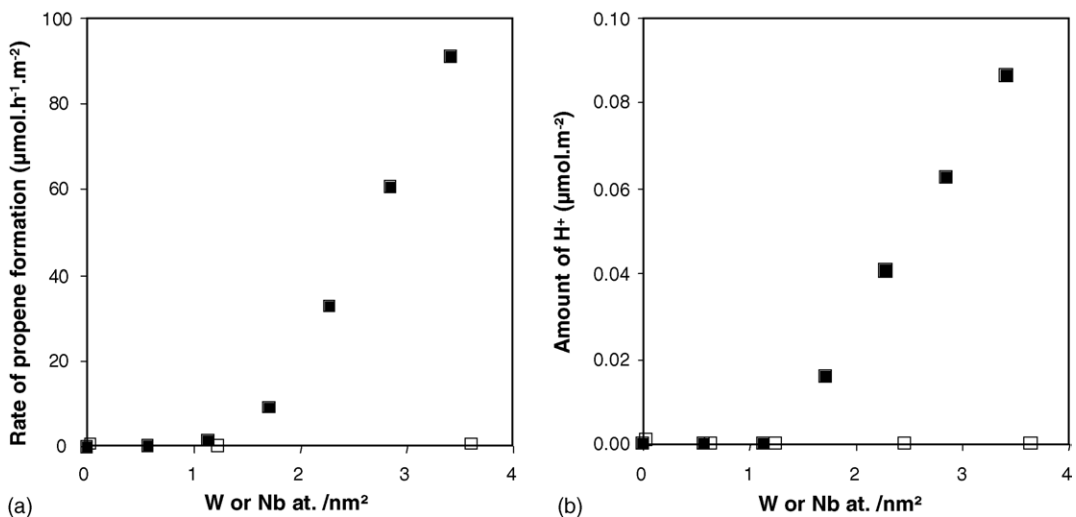


Fig. 8. (a) Propene formation rate measured at 403 K vs. W (■) or Nb (□) surface density; (b) evolution of the abundance of Brønsted acid sites, measured by lutidine desorption at 573 K, as a function of W (■) or Nb (□) surface density.

to the formation of “extensively” polymerized niobates species for low Nb surface density.

5. Conclusions

The development of acidity and catalytic activity for propan-2-ol dehydration with increasing the surface density of the deposited phase was studied for two series of catalysts, WO_x/TiO_2 and $\text{NbO}_x/\text{TiO}_2$.

Characterization of both systems by X-ray diffraction and Raman spectroscopy studies did not show evidence of bulk metal oxide formation.

The acidity was monitored by adsorption of 2,6-dimethylpyridine (2,6-lutidine) followed by infrared spectroscopy. Relatively strong Brønsted acid sites were detected for WO_x/TiO_2 catalysts. These sites only developed above a threshold of $1.1 \text{ W atom nm}^{-2}$. For $\text{NbO}_x/\text{TiO}_2$ catalysts, only moderate Brønsted acidity developed with Nb addition.

The catalytic activity was tested for the reaction of isopropanol dehydration. At a reaction temperature of 403 K, WO_x/TiO_2 catalysts were inactive for a surface density of $\text{W} \leq 1.1 \text{ W atom nm}^{-2}$. Above this loading, the activity increased progressively with increasing W content. Similar evolution was observed for the abundance of relatively strong Brønsted acid sites (i.e., able to retain 2,6-lutidine at 573 K).

In contrast, $\text{NbO}_x/\text{TiO}_2$ catalysts were essentially inactive at this reaction temperature and a higher reaction temperature (473 K) was required to reach a comparable catalytic activity. No threshold of Nb loading for the development of catalytic activity was observed. Similar behavior was evidenced for the abundance of medium strength Brønsted acid sites (able to retain 2,6-lutidine at 523 K). For both systems, a direct correlation between the catalytic activity and the abundance of Brønsted acid sites was observed.

Acknowledgements

The Van Gogh exchange Program is gratefully acknowledged for a grant. Thanks are due to Mrs. M.-N. Metzner (Lab. SIFCOM, UMR CNRS 6176, ENSICAEN, Université de Caen) for performing the XRD measurements.

References

- [1] T. Yamagishi, Y. Tanaka, K. Tanabe, *J. Catal.* 65 (1980) 442.
- [2] S. Meijers, L.H. Gielgens, V. Ponec, *J. Catal.* 156 (1995) 147.
- [3] D.G. Barton, S.L. Soled, G.D. Meitzner, G.A. Fuentes, E. Iglesias, *J. Catal.* 181 (1999) 57.
- [4] M. Scheithauer, T.-K. Cheung, R.E. Jentoft, R.K. Grasselli, B.C. Gates, H. Knözinger, *J. Catal.* 180 (1998) 1.
- [5] S. Eibl, R.E. Jentoft, B.C. Gates, H. Knözinger, *Phys. Chem. Chem. Phys.* 2 (2000) 2565.
- [6] J.-M. Jehng, I.E. Wachs, *Catal. Today* 8 (1990) 37.
- [7] L.L. Murrell, D.C. Grenoble, C.J. Kim, N.C. Dispenziere Jr., *J. Catal.* 107 (1987) 463.
- [8] C.L.T. da Silva, V.L.L. Camorin, J.L. Zötin, M.L.R.D. Pereira, A.C. Fara Jr., *Catal. Today* 57 (2000) 209.
- [9] S.B. Bukallah, Ph.D. Thesis, Vanderbilt University, Nashville, USA, 2000.
- [10] P. Viparelli, P. Ciambelli, L. Lisi, G. Ruoppolo, G. Russo, J.C. Volta, *Appl. Catal. A* 184 (1999) 291.
- [11] M. Shirai, N. Ichikuni, K. Asakura, Y. Iwasawa, *Catal. Today* 8 (1990) 57.
- [12] T. Onfroy, G. Clet, M. Houalla, *Chem. Commun.* (2001) 1378.
- [13] T. Onfroy, G. Clet, M. Houalla, *J. Phys. Chem. B* 109 (2005) 3345.
- [14] T. Onfroy, G. Clet, S.B. Bukallah, D.M. Hercules, M. Houalla, *Catal. Lett.* 89 (2003) 15.
- [15] T. Onfroy, G. Clet, M. Houalla, *J. Phys. Chem. B* 109 (2005) 14588.
- [16] F. Hilbrig, H. Schmelz, H. Knozinger, in: L. Guczi, F. Solymosi, P. Tetenyi (Eds.), *Proceedings of the 10th ICC*, Budapest, July 19–24, 1992, *Stud. Surf. Sci. Catal.*, vol. 75, Elsevier, Amsterdam, 1993, p. 1351.
- [17] P. Patrono, A. La Ginestra, G. Ramis, G. Busca, *Appl. Catal. A* 107 (1994) 249.
- [18] G. Ramis, G. Busca, C. Cristiani, L. Lietti, P. Forzatti, F. Bregani, *Langmuir* 8 (1992) 1744.
- [19] A. Gutiérrez-Alejandre, P. Castillo, J. Ramirez, G. Ramis, G. Busca, *Appl. Catal. A* 216 (2001) 181.
- [20] J. Engweiler, J. Harf, A. Baiker, *J. Catal.* 159 (1996) 259.
- [21] J. Datka, A.M. Turek, J.-M. Jehng, I.E. Wachs, *J. Catal.* 135 (1992) 186.
- [22] R.A. Spurr, H. Myers, *Anal. Chem.* 29 (1957) 760.
- [23] T. Onfroy, G. Clet, M. Houalla, *Microporous Mesoporous Mater.* 82 (2005) 99.
- [24] N. Vaidyanathan, M. Houalla, D.M. Hercules, *Surf. Interface Anal.* 26 (1998) 415.
- [25] B. Zhao, X. Xu, J. Gao, Q. Fu, Y. Tang, *J. Raman Spectrosc.* 27 (1996) 549.
- [26] R.M. Pittman, A.T. Bell, *J. Phys. Chem.* 97 (1993) 12178.
- [27] R.B. Quincy, M. Houalla, D.M. Hercules, *Fresenius J. Anal. Chem.* 346 (1993) 676.
- [28] J.-M. Jehng, I.E. Wachs, *J. Phys. Chem.* 95 (1991) 7373.
- [29] N. Vaidyanathan, D.M. Hercules, M. Houalla, *Anal. Bioanal. Chem.* 373 (2002) 547.
- [30] S.S. Chan, I.E. Wachs, L.L. Murrell, L. Wang, W.K. Hall, *J. Phys. Chem.* 88 (1984) 5831.
- [31] M.A. Vuurman, I.E. Wachs, A.M. Hirt, *J. Phys. Chem.* 95 (1991) 9928.
- [32] R. Brayner, F. Bozon-Verduraz, *Phys. Chem. Chem. Phys.* 5 (2003) 1457.
- [33] J.-M. Jehng, I.E. Wachs, *Chem. Mater.* 3 (1991) 100.
- [34] J.-M. Jehng, I.E. Wachs, *J. Mol. Catal.* 67 (1991) 369.
- [35] C. Lahousse, A. Aboulayt, F. Maugé, J. Bachelier, J.-C. Lavalley, *J. Mol. Catal.* 84 (1993) 283.
- [36] A. Travert, O.V. Manoilova, A.A. Tsyganenko, F. Maugé, J.-C. Lavalley, *J. Phys. Chem. B* 106 (2002) 1350.
- [37] J.R. Sohn, J.H. Bae, *Kor. J. Chem. Eng.* 17 (2000) 86.